Realization of high-performance blue organic light-emitting diodes using multi-emissive layers

Ju-An Yoon[1], You-Hyun Kim[1], Nam Ho Kim[1], Chul Gyu Jhun[1], Song Eun Lee[2], Young Kwan Kim[2], Fu Rong Zhu[4], and Woo Young Kim[1,3*]

[1]*Department of Green Energy & Semiconductor Engineering, Hoseo University, Asan 330-713, South Korea*

[2]*Department of Information Display, Hongik University, Seoul 121-791, South Korea*

[3]*Department of Engineering Physics, McMaster University, Hamilton, Ontario L8S 4L7, Canada*

[4]*Department of Physics, Hong Kong Baptist University, Hong Kong, China*

[*]*Corresponding author: jjuan25@naver.com*

Received September 30, 2013; accepted December 3, 2013; posted online January 8, 2014

High-performance blue organic light-emitting diodes (OLEDs) are developed. A concept of using multiple-emissive layer (EML) configuration is adopted. In this letter, bis(2-methyl-8-quinolinolate)-4-(phenylphenolato)Al (BAlq) and 9,10-di(naphtha-2-yl)anthracene (ADN), which serve n- and p-type EMLs, respectively, are used to evaluate and demonstrate the multi-EML concept for blue OLEDs. The thickness effect of individual EMLs and the number of EMLs, e.g., triple and quadruple EML components, on the power efficiency of blue OLEDs are systematically investigated. To illustrate the point, the total thickness of the emissive region in different blue OLEDs are kept contact at 30 nm for comparison. The power efficiency of blue OLEDs with a quadruple EML structure of BAlq/ADN/BAlq/ADN is about 40% higher than that of blue OLEDs having a single EML unit. The Commission Internationale deL'eclairage color coordinates of multi-EML OLEDs have values that represent the average of blue emissions from individual EMLs of BAlq and ADN.

OCIS codes: 230.0230, 230.3670, 230.0250, 160.4890, 130.5990.
doi: 10.3788/COL201412.012302.

Organic light-emitting diodes (OLEDs) are attracting worldwide interest because of their display advantages, such as reduced power consumption, compatibility with flexible substrates, high color rendering index, high contrast, and wide viewing angle[1,2]. White OLEDs (WOLEDs) have emerged as a strong candidate for next-generation flat-panel displays and solid-state lighting[3−5]. High-performance WOLEDs are developed through material innovation and device optimization. The power efficiency of WOLEDs could achieve more than 40 lm/W at 100 cd/m^2[3]. A semitransparent WOLED with a visible-light transparency of >50%, an almost identical power efficiency of 11 lm/W measured at 100 cd/m^2, and the similar Commission Internationale deL'eclairage (CIE) coordinates of (0.36, 0.43) and (0.38, 0.46) from both sides has been demonstrated recently[6]. Although many studies have improved the overall power efficiency of WOLEDs, the development of efficient blue OLEDs remains a challenge[7−9]. The blue OLED component plays an important role in determining high-performance WOLED lighting. Various methods have been developed to optimize the electrical and optical performances of blue OLEDs. Emitters are replaced from fluorescent to phosphorescent materials[10]. The charge carrier ratio is balanced in the EML[11]. A better surface texture is designed for improving external quantum efficiency[12,13]. Multi-emissive layer (EML) structures have been used for OLEDs[14,15], because their chromaticity can be tuned by varying the thicknesses and order of EMLs; they could also produce higher efficiency through emission in different EMLs that occurs at different regions of visible spectra[16].

In this letter, blue OLEDs using two fluorescent organic semi-conductor materials of bis(2-methyl-8-quinolinolate)-4-(phenylphenolato)Al (BAlq) and 9,10-Di(naphtha-2-yl)anthracene (ADN) for single EML were fabricated under different order and number of layers to obtain optimized electrical and optical performances. Power efficiency and current density–voltage–luminous (I–V–L) characteristics were observed through considering the effects of multi-EML structures and the variation of the recombination region in EML.

ITO-coated glass was cleaned in ultrasonic bath by regular sequences in acetone, methanol, diluted water, and isopropyl alcohol. The pre-cleaned ITO was treated by O_2 plasma under the conditions of 2×10^{-2} Torr and 125 W for 2 min[17]. Blue OLEDs were fabricated by high-vacuum (1.0×10^{-6} Torr) thermal evaporation using N,N'-bis-(1-naphyl)-N, N'-diphenyl-1, 1'-biphenyl-4, 4'- diamine (NPB), BAlq, ADN, 4, 7-di-phenyl-1, 10-phenanthroline (Bphen), Li quinolate (Liq), and Al, which were deposited at evaporation rates of 0.1, 0.05, 0.05, 0.1, 0.01, and 0.5 nm/s, respectively.

The molecular structures of the blue chromophores used in the blue OLEDs are shown in Fig. 1. The basic structure of blue OLED with multi-EML is ITO/NPB/single, triple, or quadruple EML using BAlq and ADN/Bphen as electron transport layer/Liq/Al cathode. ITO serves as front anode, a layer of NPB is the hole-transporting layer, and Liq is the electron transporting layer. Four types of blue OLEDs with different EMLs of BAlq, ADN, BAlq/ADN/BAlq, and BAlq/ADN/BAlq/ADN were fabricated. The thickness

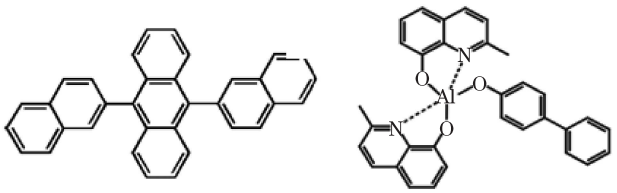

Fig. 1. Molecular structures of blue emissive materials.

of individual EML in the stack of EMLs was optimized by keeping a total thickness of the emissive region of 30 nm. A summary of OLED device parameters is shown in Table 1.

With various DC voltage bias, the optical and electrical properties of blue OLEDs, such as current density, luminance, power efficiency, CIE$_{xy}$ coordinates, and electroluminescence (EL) spectra, were measured with Keithley 238, LMS PR-650 spectrophotometer and colorimeter, and the I–V–L system.

Figure 2 shows current density as a function of voltage for each device. Blue OLEDs with single EML of ADN (device A) and BAlq (device B) are fabricated. ADN is a p-type-emitting material with high hole mobility, while BALq is an n-type-emitting material. The results show that blue OLEDs with ADN have the highest current density, whereas device B has the lowest current density, because p-type semiconductor has more electron affinity than n-type one. The schematic energy band diagrams of devices A to D are shown in Fig. 3. The hole injection barriers of devices A and B are 0.4 and 0.7 eV, and their electron injection barriers are 0.4 and 0.1 eV, respectively. Hole mobility and hole injection barrier are usually more effective than electron mobility and electron injection barrier on the electrical and optical performances of OLEDs[18]. Devices C and D are fabricated with triple and quadruple EML structures using two different blue emissive materials of ADN and BAlq, and charge-blocking structures are spontaneously formed between these EMLs. Device D has wider ADN region than device C. However, Devices C and D have similar current density. This result is contradicted to that p-type emissive material device has current density higher than n-type emissive material device. The result can be explained as that devices C and D have the same hole injection barrier, but device D has 0.3 eV higher electron injection barrier than device C. In addition, electrons and holes are confined at EML by charge-blocking structure to inhibit the current flow in EML[19].

Figure 4(a) shows the plot of power efficiency as a function of current density for different blue OLED devices. The power efficiencies of devices A to D measured at 20 mA/cm^2 are 1.54, 1.82, 2.02, and 2.16 lm/W, respectively.

Devices C and D have relatively higher power efficiencies than devices A and B at low current density. Especially, device D has the highest power efficiency, which is almost 40% higher than that of device A. The power efficiency of blue OLED device D with a multi-EML structure is determined by two factors. The first factor is that the emissive region of device D is evenly formed by ADN and BAlq. As a result, the power efficiency is enhanced, because ADN and BAlq are emissive at different wavelengths. The second factor is that device D has charge-blocking sutrctures at the interface between ADN and BAlq. The transportation of hole and electron from anode to cathode is suppressed by charge-blocking structures and high-charge injection barrier when triple

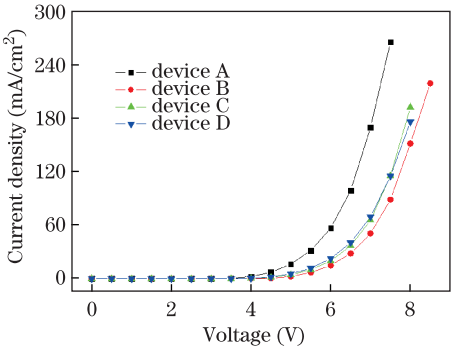

Fig. 2. Current density as a function of operation voltage measured for blue OLED devices A to D.

Table 1. Layer Structures of Blue OLED Devices A to D

Device	HTL	EML	ETL	EIL	Cathode
Device A	NPB(70 nm)	ADN(30 nm)	Bphen(30 nm)	Liq(2 nm)	Al(120 nm)
Device B	NPB(70 nm)	BAlq(30 nm)	Bphen(30 nm)	Liq(2 nm)	Al(120 nm)
Device C	NPB(70 nm)	BAlq(10 nm)/ADN(10 nm)/BAlq(10 nm)	Bphen(30 nm)	Liq(2 nm)	Al(120 nm)
Device D	NPB(70 nm)	BAlq(7.5 nm)/ADN(7.5 nm)/BAlq(7.5 nm)/ADN(7.5 nm)	Bphen(30 nm)	Liq(2 nm)	Al(120 nm)

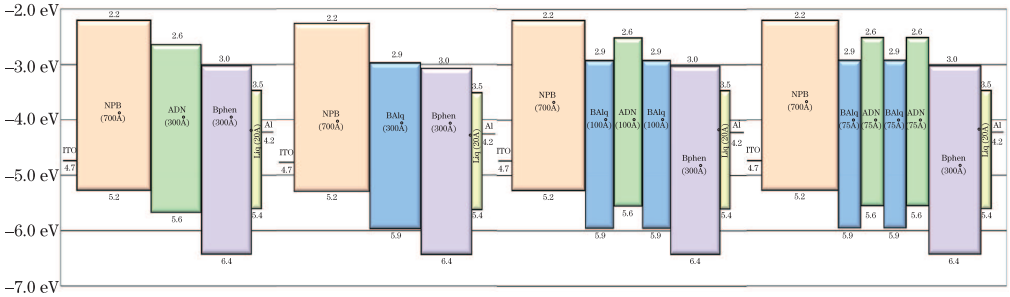

Fig. 3. Schemetic energy band diagrams of blue OLED devices A to D.

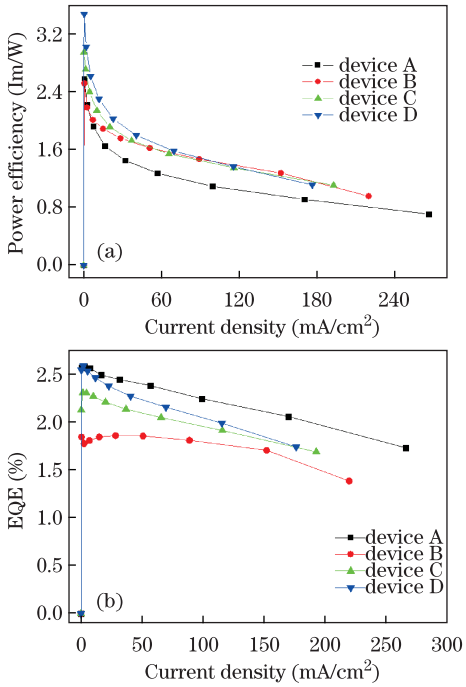

Fig. 4. (a) Power efficiency-current density characteristics and (b) external quantum efficiency-current density characteristics measured for devices A to D.

and quadruple EMLs are used. A 0.7-eV gap in HOMO energy levels between NPB and BAlq induces a decrease in hole injection, whereas a 0.3-eV difference in HOMO energy levels between ADN and BAlq increases hole trapping because of the difference in the hole and electron mobility in EML. Meanwhile, a 0.4-eV electron injection barrier between Bphen and BAlq is lower than the hole injection barrier, and a 0.3-eV gap in LUMO energy levels between ADN and BAlq leads to confine electrons injected from cathode. With the increase of bias voltages, the injected electrons from cathode are recombined with trapped holes owing to the 0.7-eV hole injection barrier of HOMO energy levels between NPB and BAlq. This charge transport mechanism is the major factor that influences the balance of hole and electron recombination in EML. The charge balance is improved at EML by the charge blocking of HOMO and LUMO.

Device D has higher power efficiency than device C, because device D has two charge-blocking structures that enhance recombination, whereas device C has only one charge-blocking structure in HOMO and LUMO levels between the ADN and BAlq interface. However, device C has better efficiency roll-off than device D. The efficiency roll-off is usually observed because of the difference in hole and electron mobility in EMLs. In OLEDs with quantum well structure in EML, such as devices C and D, a fast roll-off behavior is observed because of the imbalance of hole–electron current in EML[20−22]. Consequently, device C with triple EML would provide higher probability of electron–hole recombination than device D with quadruple EML for OLEDs with a constant EML thickness of 30 nm.

Figure 4(b) shows the plot of external quantum efficiency as a function of current density for different blue OLEDs. The external quantum efficiencies of devices A to D measured at 20 mA/cm^2 are 2.47%, 1.85%, 2.22%, and 2.41%, respectively. External quantum efficiency has different trend compared with power efficiency. The power efficiency is calculated by considering human visual characteristics, whereas the external quantum efficiency does not consider these characteristics. BAlq is emitted at nearby green region with excellent human visual characteristics. Thus, more emission at BAlq happens, and more power efficiencies and less external quantum efficiency are obtained.

Figure 5(a) shows EL spectra of devices A to D, and their major peaks appear at 460, 488, 476, and 476 nm, respectively. The blue emission peaks of devices C and D in EL spectra are observed between those of devices A and B, which appear from the pure emission of ADN and BAlq. Figure 5(b) shows the un-normalized EL spectra of devices A to D and the fitting EL spectra that normalize the sum of the blue emission peaks of devices A and B. Their shape of fitting EL spectra appears almost similar to those of devices C and D. As mentioned above, the blue emission peaks of devices C and D occur at the middle of the single emission of ADN and BAlq. The intensity of BAlq is higher than that of ADN, which is caused by charge-blocking structures. Therefore, electron-blocking structures are more effective in charge balancing compared with hole-blocking structures.

Figure 6 presents the CIE$_{xy}$ coordinates of devices A to D, i.e., (0.157, 0.146), (0.200, 0.344), (0.189, 0.264), and (0.184, 0.263) at 5 V, respectively. The CIE$_{xy}$ coordinates of devices C and D are mostly located in the middle of devices A and B, but those of device C is closely located to the CIE$_{xy}$ coordinates of device B compared with those of device D. These results are attributed to the electron–hole recombination at the BAlq layer nearby cathode electrode because of the different mobility of hole and electron.

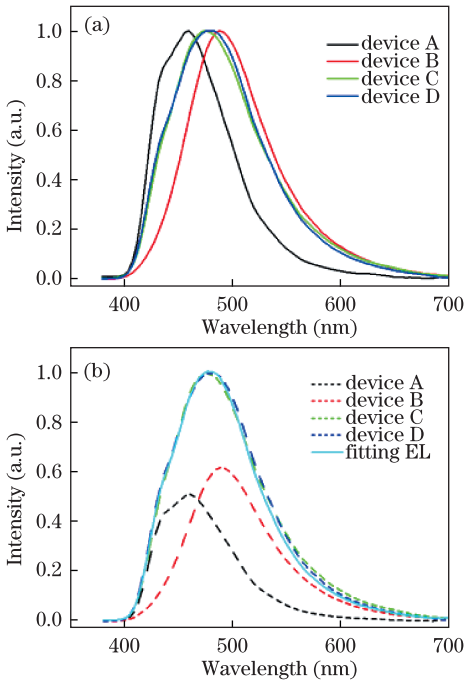

Fig. 5. (a) Comparison of EL spectra measured for blue OLED devices A to D at 5.0 V; (b) corresponding theoretical fitted EL spectra for the devices.

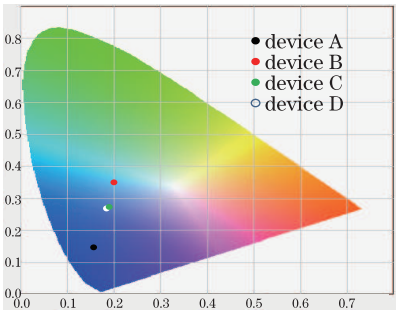

Fig. 6. CIE$_{xy}$ coordinates of blue OLED devices A to D measured at an operation voltage of 5 V.

In conclusion, the performances of single and multiple-EML blue OLEDs, fabricated using BAlq- and ADN-emitting materials, are analyzed. The effects of different combinations of BAlq and ADN EMLs on the power efficiency of the blue OLEDs are investigated. The power efficiency of the blue OLEDs with quadruple EML is about 40% higher than OLED with a single ADN EML. The efficiency roll-off of the blue OLEDs with a constant EML thickness of 30 nm is improved through optimizing the EML structure. OLEDs with EMLs render the expansion of recombination zone throughout the emission region formed by ADN and BAlq, which is demonstrated by the characteristic emission peaks from ADN and BAlq. Device D, with two HOMO and LUMO charge-blocking structures using BAlq and ADN as EML materials, shows the best electrical and optical performances. Phosphorescent blue OLEDs with multi-EML structures will be fabricated to examine charge-blocking structure and triplet energy transfer for the performance optimization of blue OLEDs prior to obtaining WOLED with a host–guest system in near future.

This research project entitled "Development of High-efficient White Organic Light-emitting Diodes for Lighting Application" was supported by Korea Industry Foundation.

References

1. C. W. Tang and S. A. VanSlyke, Appl. Phys. Lett. **51,** 913 (1987).
2. T. Mori, T. Itoh, and T. Mizutani, J. Photopolym. Sci. Technol. **17,** 301 (2004).
3. S. Reineke, F. Lindner, G. Schwartz, N. Seidler, K. Walzer, B. Lüssem, and K. Leo, Nature **459,** 234 (2009).
4. G. Gu, P. E. Burrows, S. Venkatesh, S. R. Forrest, and M. E. Thompson, Opt. Lett. **22,** 172 (1997).
5. D. Song, S. Zhao, and H. Aziz, Adv. Funct. Mater. **21,** 2311 (2011).
6. W. H. Choi, H. L. Tam, F. R. Zhu, D. G. Ma, H. Sasabe, and J. Kido, Appl. Phys. Lett. **102,** 153308 (2013).
7. B. W. D'Andrade and S. R. Forrest, Adv. Mater. (Weinheim, Ger.) **16,** 1585 (2004).
8. B. C. Krummacher, V. E. Choong, M. K. Mathai, S. A. Choulis, F. So, F. Jermann, T. Fiedler, and M. Zachau, Appl. Phys. Lett. **88,** 113506 (2006).
9. B. W. D'Andrade, R. J. Holmes, and S. R. Forrest, Adv. Mater. (Weinheim, Ger.) **16,** 624 (2004).
10. J. Shinar, *Organic Light-Emitting Devices* (Springer Press, New York, 2004).
11. E. Gautier-Thianche, C. Sentein, A. Lorin, C. Denis, P. Raimond, and J. M. Nunzi, J. Appl. Phys. **83,** 4236 (1998).
12. C. Hubert, C. Fiorini-Debuisschert, I. Hassiaoui, L. Rocha, P. Raimond, and J. M. Nunzi, Appl. Phys. Lett. **87,** 191105 (2005).
13. S. Huang, Z. Ye, J. Lu, Y. Su, C. Chen, and G. He, Chin. Opt. Lett. **11,** 062302 (2013).
14. B. W. D'Andrade, J. Brooks, V. Adamovich, M. E. Thompson, and S. R. Forrest, Adv. Mater. (Weinheim, Ger.) **14,** 1032 (2002).
15. S. Tokito, T. Lijima, T. Tsuzuki, and F. Sato, Appl. Phys. Lett. **83,** 2459 (2003).
16. G. Cheng, Y. Zhang, Y. Zhao, Y. Lin, C. Ruan, S. Liu, T. Fei, Y. Ma, and Y. Cheng, Appl. Phys. Lett. **89,** 043504 (2006).
17. C. C. Wu, J. C. Sturm, and A. Khan, Appl. Phys. Lett. **70,** 1348 (1997).
18. W. Culligan, A. C. A. Chen, J. U. Wallace, K. P. Klubek, C. W. Tang, and S. H. Chen, Adv. Funct. Mater. **16,** 1481 (2006).
19. S. H. Kim, J. Jang, J.-M. Hong, and J. Y. Lee, Appl. Phys. Lett. **90,** 173501 (2007).
20. S. Liu, B. Li, L. Zhang, and S. Yue, Appl. Phys. Lett. **98,** 163301 (2011).
21. T. J. Park, W. S. Jeon, J. W. Choi, R. Pode, K. Jang, and J. H. Kwon, Appl. Phys. Lett. **95,** 103303 (2009).
22. Y. Qiu, Y. Gao, P. Wei, and L. Wang, Appl. Phys. Lett, **80,** 2628 (2002).